 SL, vol.6, no.2, pp.39-46, 2011

# Intravascular Ultrasound (IVUS)-Based Computational Modeling and Planar Biaxial Artery Material Properties for Human Coronary Plaque Vulnerability Assessment

**Mingchao Cai**[1], **Chun Yang**[2], **Mehmet H. Kural**[1], **Richard Bach**[3]
**David Muccigrosso**[4], **Deshan Yang**[5], **Jie Zheng**[4], **Kristen L. Billia**[1]
**Dalin Tang**[1,6]

**Abstract:** Image-based computational modeling has been introduced for vulnerable atherosclerotic plaques to identify critical mechanical conditions which may be used for better risk assessment and rupture predictions. In vivo patient-specific coronary plaque models are lagging due to limitations on non-invasive image resolution, flow data, and vessel material properties. We propose a procedure where intravascular ultrasound (IVUS) imaging, biaxial mechanical testing and computational modeling are combined together to acquire better and more complete plaque data and make more accurate plaque vulnerability assessment and predictions.

**Keywords:** Coronary artery; cardiovascular; fluid-structure interaction; atherosclerotic plaque rupture, IVUS.

## 1 Introduction

Atherosclerotic plaques may rupture without warning and cause acute cardiovascular syndromes such as heart attack and stroke. It is commonly believed that plaque rupture may be linked to critical stress/strain conditions. Image-based computational models have been developed by several groups combining mechanical analysis with image technology aiming to identify critical flow and stress/strain con-

[1] Worcester Polytechnic Institute, Worcester, MA 01609
[2] School of Mathematical Sciences, Beijing Normal University, Key Laboratory of Mathematics and Complex Systems, Ministry of Education, Beijing, 100875, China
[3] Cardiovascular Division, Washington University School of Medicine, Saint Louis, MO 63110, USA
[4] Mallinckrodt Institute of Radiology, Washington University School of Medicine, St. Louis, MO 63110 USA
[5] Radiation Oncology, Washington University School of Medicine, Saint Louis, MO 63110, USA
[6] Corresponding author, dtang@wpi.edu

ditions which may be related to possible plaque rupture [Bluestein et al. (2008); Chandran et al. (2006); Groen et al. (2007); Holzapfel et al. (2004); Li et al. (2007); Liang, Zhu, and Friedman, (2008); Tang (2006); Tang et al. (2005); Yang et al. (2008, 2009)]. However, existing in vivo 3D plaque models are mostly for carotid plaques based on magnetic resonance imaging (MRI) data. Similar models for coronary plaques based on in vivo image data is lacking in the current literature because clinical recognition of vulnerable coronary plaques has remained challenging and beyond the capability of non-invasive diagnostic imaging such as MRI and CT coronary angiography. Coronary imaging is more difficult because: a) coronary arteries move with the pumping heart constantly; b) coronary artery has smaller dimensions compared to carotid arteries; c) coronary arteries are not as accessible as carotid arteries; and d) plaque components are not reliably delineated as in carotid arteries. Traditional invasive x-ray angiography can delineate luminal stenosis, but not plaque components. Intravascular ultrasound (IVUS) imaging with tissue characterization represents the most promising and potentially clinically relevant technique for recognition of vulnerable plaques in vivo in patients [Mintz et al. (2001)].

A modeling approach is proposed to develop 3D in vivo IVUS-based models with fluid-structure interactions (FSI), cyclic bending and anisotropic properties to perform mechanical analysis for human coronary atherosclerotic plaques. The procedure includes a) IVUS acquisition of coronary plaque morphology and blood flow and pressure information; b) CT coronary angiography and 3D reconstruction for coronary motion and curvature; c) biaxial mechanical testing of coronary plaque material properties; d) 3D computational modeling based on data acquired in a)-c). Cyclic bending represents the bending caused by cardiac motion and is included in the FSI model to evaluate its impact on stress conditions in coronary plaques. Anisotropic material models will be used for the vessel for more realistic modeling and more accurate computational flow and stress/strain predictions.

## 2 Data acquisition, models and methods

### *2.1 IVUS plaque image, flow velocity and pressure data acquisition*

3D IVUS data sets will be acquired during cardiac catheterization from patients after voluntary informed consent. For IVUS image acquisition, a 20-MHz, 2.9F phased-array Eagle Eye Gold IVUS catheter (Volcano Corp., Rancho Cordova, CA) was positioned 2 cm beyond a stenosis in the mid segment of the right coronary artery. A pullback at 0.5mm/s was performed to 2 cm proximal to the lesion for recording digitized cross-sectional IVUS images. The catheter orientation is fixed at the proximal interface with the imaging console and the distal tip is con-

strained by the coronary guidewire that remains stationary in the monorail lumen. A Combo-Wire XT 9500 (Volcano Therapeutics, Inc.) 0.014-inch guide-wire with a Doppler flow velocity sensor at the tip was used (figure above). The pressure sensor is 15 mm offset from the flow sensor. The measurements were recorded digitally onto a ComboMap (Volcano Therapeutics, Inc.) console for offline analysis. Measurement of intracoronary flow velocity and blood pressure was acquired at baseline. An average of 5 beats was used to calculate average peak velocity (APV) at baseline. Blood pressure data was extracted from Pd, an averaged pressure recorded on the pressure sensor. Although there is an offset between two sensors, the Pd should be very close to the pressure around the flow sensor. Figure 1 shows 3 sample IVUS slices, segmented contours and screen display of flow and pressure data.

The traditional x-ray angiogram (Allura Xper FD10 System, Philips, Bothel, WA) was obtained prior to the pullback of the IVUS catheter to determine the location of the coronary artery stenosis in patients (Fig. 2). Because this imaging modality can demonstrate the dynamic phasic changes of the coronary artery tree during the cardiac cycle with a high frame rate (30 frames / sec), we used x-ray angiographic data for the determination of the stenosis segment movement and curvature.

(a) Sample IVUS slices out of a 195-slice set

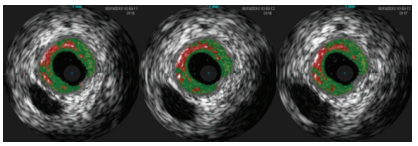

(b) Corresponding segmented slices S115-S117.

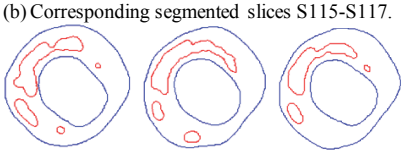

(c) IVUS Volcano Screen Display of Flow Velocity and Blood Pressure Using a Combo-Wire.

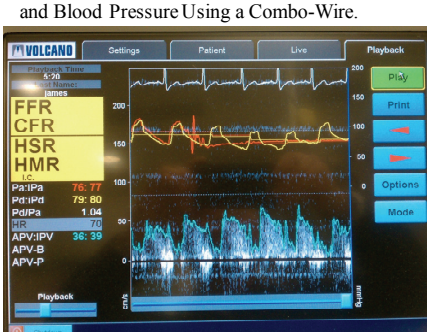


Figure 1: Sample IVUS slices and screen display showing on-site blood pressure and flow velocity.

### *2.2 Mechanical Testing and Isotropic and Anisotropic Material Models*

A custom planar biaxial test device was used under stress control to obtain stress and strain measurements over a wide range of ratios of stress along the longitudinal and circumferential axes of arterial specimens splayed open to form square

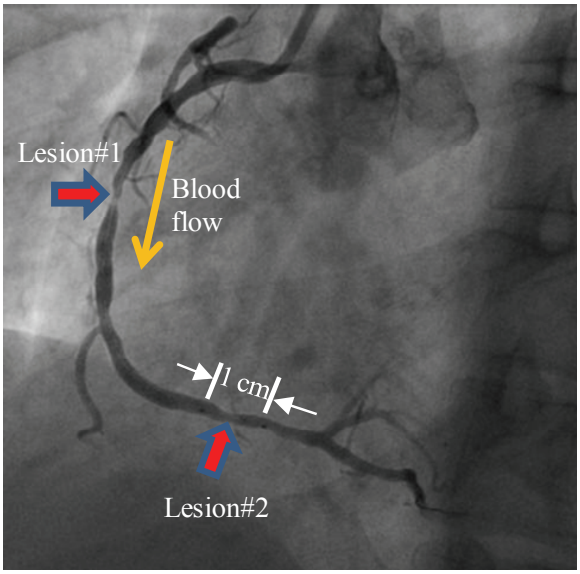


Figure 2: X-Ray angiographic image used to determine location of the myocardium and patient-specific curvature variations.

samples. The forces along the axes were measured via two torque transducers (effective resolution ∼0.02N) to determine the stress. Four graphite particles attached to the sample were tracked by a CCD camera to determine 2D strain (640 x 480 pixels; effective resolution ∼0.07% strain). Four non-fixed human coronary arteries mounted on the biaxial test device using tethered hooks and submerged in saline. The applied maximum longitudinal: circumferential stress ratios were 1:1, 0.7:1, 0.5:1, 1:0.7 and 1:0.5. Based on average stress in the vessel walls at systolic pressure, the maximum engineering stress applied was 250kPa. A modified Mooney-Rivlin (M-R) model [Yang et al. (2009)] was fit to the four of the loading protocols:

$$\Psi = c_1(I_1 - 3) + D_1[\exp(D_2(I_1 - 3)) - 1] + \frac{K_1}{2K_2}[\exp(K_2(I_4 - 1)^2 - 1)] \tag{1}$$

where $I_1 = \sum C_{ii}$ is the first strain invariant, $I_4 = C_{ij}(n_c)_i(n_c)_j$, $C_{ij}$ is the Cauchy–Green deformation tensor, $n_c$ is the circumferential direction of the vessel, $c_1$, $D_1$, $D_2$, and $K_1$ and $K_2$ are material constants. Setting $K_1$=0 gives the isotropic model. The fifth protocol was reserved to verify the predictive capability of the constitutive equation.

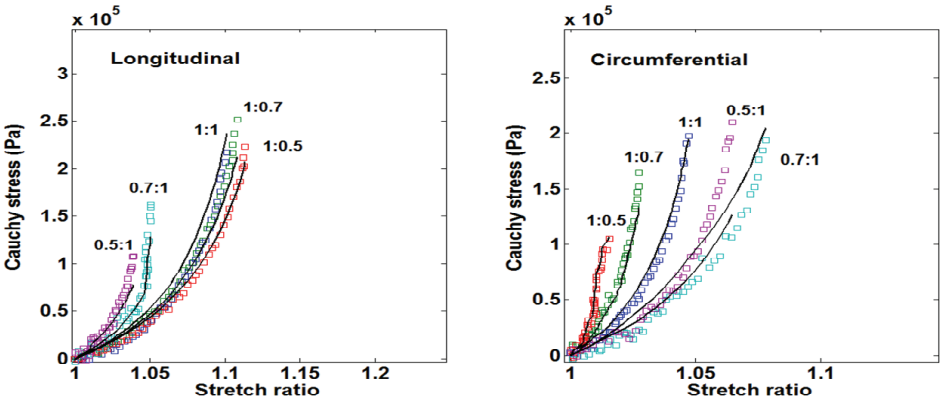


Figure 3: Biaxial mechanical data for a left coronary artery (LCA) data and fit using the modified Mooney-Rivlin model.

### *2.3 3D FSI model construction with cyclic bending and boundary conditions*

3D anisotropic and isotropic multi-component FSI models were constructed using established procedures [Yang et al. (2009)] to calculate flow and stress/strain distributions and evaluate the effects of anisotropic properties and other risk indicators. Blood flow was assumed to be laminar, Newtonian, and incompressible. The Navier-Stokes equations with arbitrary Lagrangian-Eulerian formulation were used as the governing equations. On-site pressure conditions from IVUS measurements were prescribed at both inlet and outlet. No-slip conditions and natural traction equilibrium conditions are assumed at all interfaces. Putting these together, we have:

$$\rho(\partial u/\partial t + ((u-u_g)\cdot\nabla)\mathbf{u}) = -\nabla p + \mu\nabla^2\mathbf{u}, \tag{2}$$

$$\nabla\cdot\mathbf{u} = 0, \tag{3}$$

$$\mathbf{u}\,|_\Gamma = \partial\mathbf{x}/\partial t, \quad \partial\mathbf{u}/\partial n|_{inlet,outlet} = 0, \tag{4}$$

$$p|_{inlet} = p_{in}(t), \quad p|_{outlet} = p_{out}(t), \tag{5}$$

$$\rho v_{i,tt} = \sigma_{ij,j}, \quad i,j = 1,2,3; \quad \text{sum over } j, \tag{6}$$

$$\varepsilon_{ij} = (v_{i,j} + v_{j,i} + v_{\alpha,i}v_{\alpha,j})/2, \quad i,j,\alpha = 1,2,3, \tag{7}$$

$$\sigma_{ij}\cdot n_j|_{out\_wall} = 0, \tag{8}$$

$$\sigma^r_{ij}\cdot n_j|_{interface} = \sigma^s_{ij}\cdot n_j|_{interface}, \tag{9}$$

where $\mathbf{u}$ and p are fluid velocity and pressure, $\mathbf{u}_g$ is mesh velocity, $\mu$ is the dynamic viscosity, $\rho$ is density, $\Gamma$ stands for vessel inner boundary, $f_{,j}$ stands for derivative of the function f with respect to the jth variable, $\sigma$ is stress tensor (superscripts indicate different materials), $\varepsilon$ is strain tensor, $\mathbf{v}$ is solid displacement vector, superscript letters "r" and "s" were used to indicate different materials. For simplicity, all material densities were set to 1 g·cm$^{-3}$ in this paper.

## 3 Results

Various FSI models reconstructed from IVUS were used to quantify effects of different model assumptions on flow and stress-strain distributions. Effect of the following factors will be investigated: a) plaque morphology, including varying plaque cap, lipid core size and position; b) material properties, isotropic vs. anisotropic; stiffer vs. softer; diseased artery vs. healthy artery; c) pressure condition: IVUS-measured pressure vs. arm pressure; d) heart motion as simulated by cyclic bending. Figure 4 gives plots of maximum principal stress (Stress-$P_1$), maximum flow shear stress and flow velocity on a cut surface from a sample plaque to give an illustration of our approach. Detailed results will be presented at the conference.

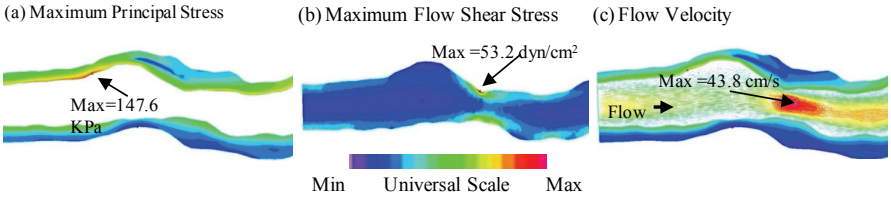


Figure 4: Illustration of modeling results: plots of maximum principal stress (Stress-$P_1$), maximum flow shear stress and flow velocity on a cut surface from a sample plaque.

## 4 Discussion and conclusion

The proposed approach provides an opportunity to improve current coronary plaque models with a) better image resolution (25 micron in-plane resolution from IVUS vs. 300 micron from in vivo MRI), b) actual measured blood pressure at the site of the lesion; and c) directly measured biaxial vessel mechanical material properties. This is only a preliminary report. Success of this project will lead to more accurate plaque vulnerability assessment and predictions for possible plaque rupture risk so that better decisions for treatment can be made leading to better public health and

reduced Medicare costs. Large scale patient studies are needed to further validate our assessment schemes.

**Acknowledgement:** This research was supported in part by NIH grant NIH/NIBIB R01 EB004759. Professor Chun Yang's research was partially supported by National Sciences Foundation of China grant 10871028.

## 5 References

Bluestein, D.; Alemu, Y.;, Avrahami, I.; Gharib, M.; Dumont, K.; Ricotta, J. J.; Einav, S. (2008): Influence of microcalcifications on vulnerable plaque mechanics using FSI modeling, *J Biomech.* vol. 41, no. 5, pp. 1111-1118.

Chandran, K. B.; Wahle, A.; Vigmostad, S. C.; Olszewski, M. E.; Rossen, J. D.; Sonka, M. (2006): Coronary arteries: imaging, reconstruction, and fluid dynamic analysis," *Crit Rev Biomed Eng*. vol. 34, no. 1, pp. 23-103, 2006.

Groen, H. C.; Gijsen, F. J.; van der Lugt, A.; Ferguson, M. S.; Hatsukami, T. S.; van der Steen, A. F., Yuan, C.; Wentzel, J. J. (2007): Plaque rupture in the carotid artery is localized at the high shear stress region: a case report. *Stroke*, 38:2379-2381.

Holzapfel, G. A.; Sommer, G.; Regitnig, P. (2004): Anisotropic mechanical properties of tissue components in human atherosclerotic plaques, *J. Biomech. Eng.* 126(5):657-665.

Li, Z. Y.; Howarth, S. P.; Tang, T.; Graves, M. J.; U-King-Im, J.; Trivedi, R. A.; KirkPatrick, P. J.; Gillard, J. H. (2007): Structural analysis and magnetic resonance imaging predict plaque vulnerability: a study comparing symptomatic and asymptomatic individuals. *J Vasc Surg.* 45(4):768-75.

Liang, Y.; Zhu, H., Friedman, M. H. (2008): Estimation of the transverse strain tensor in the arterial wall using IVUS image registration, *Ultrasound Med Biol.* 34(11):1832-45 .

Mintz, G. S.; Nissen, S. E.; Anderson, W. D.; Bailey, S. R.; Erbel, R.; Fitzgerald, P. J.; Pinto, F. J.; Rosenfield, K.; Siegel, R. J.; Tuzcu, E. M.; Yock, P. G. (2001): American College of Cardiology clinical expert consensus document on standards for acquisition, measurement and reporting of intravascular ultrasound studies (IVUS), *J Am Coll Cardiol.,* 37:1478–92.

Tang, D. (2006): Flow in Healthy and Stenosed Arteries, *Wiley Encyclopedia of Biomedical Engineering,* Article 1525, New Jersey, John Wiley & Sons, Inc..

Tang, D.; Yang, C.; Zheng, J.; Woodard, P. K.; Saffitz, J. E.; Petruccelli, J. D.; Sicard, G. A.; Yuan, C. (2005): Local maximal stress hypothesis and computational plaque vulnerability index for atherosclerotic plaque asse*ssment, Ann. Biomed.*

*Eng.,* 33(12):1789-1801.

Yang, C.; Bach, R.; Zheng, J.; El Naqa, I.; Woodard, P. K.; Teng, Z. Z.; Billiar, K. L.; Tang, D. (2009): In vivo IVUS-based 3D fluid structure interaction models with cyclic bending and anisotropic vessel properties for human atherosclerotic coronary plaque mechanical analysis, *IEEE Trans. Biomed. Engineering,* 56(10):2420-2428.

Yang, C.; Tang, D.; Kobayashi, S.; Zheng, J.; Woodard, P. K.; Teng, Z. Z.; Bach, R.; Ku, D. N. (2008): Cyclic Bending Contributes to High Stress in a Human Coronary Atherosclerotic Plaque and Rupture Risk: In Vitro Experimental Modeling and Ex Vivo MRI-Based Computational Modeling Approach, Molecular & Cellular Biomechanics, 5 (4), 259-274.